DEVELOPMENT OF LIQUID HANDLING TECHNIQUES IN MICROGRAVITY

A Final Report For NASA Grant
Number NAG8-1089

Prepared For NASA/Marshall Space Flight Center

by

Basil N. Antar

The University of Tennessee Space Institute
Tullahoma, Tennessee 37388

November 1995

TABLE OF CONTENTS

1. Introduction

A large number of experiments dealing with protein crystal growth and also with growth of crystals from solution require complicated fluid handling procedures including filling of empty containers with liquids, mixing of solutions and stirring of liquids. Such procedures are accomplished in a straight forward manner when performed under terrestrial conditions in the laboratory. However, in the low gravity environment of space, such as on board the Space Shuttle or an Earth-orbiting space station, these procedures sometimes produced entirely undesirable results. Under terrestrial conditions, liquids usually completely separate from the gas due to the buoyancy effects of Earth's gravity. Consequently, any gas pockets that are entrained into the liquid during a fluid handling procedure will eventually migrate towards the top of the vessel where they can be removed. In a low gravity environment any folded gas bubble will remain within the liquid bulk indefinitely at a location that is not known *apriori* resulting in a mixture of liquid and vapor.

There are a number of incidents cited in the literature in which, during an earth-orbital operation, the presence of gas bubbles within the liquid bulk had an adverse impact on the experiment's outcome and in some cases caused the experiments to fail. These trapped gas bubbles have been the cause of concern and frustration since the early days of low gravity research which was conducted on board Skylab. Bier et al. (1974), for instance, reported observing unexpected air bubbles in both electrophoresis chambers which hindered the successful operation of their experiment. Another early difficult experience is given in Snyder et al. (1985) during the operation of their electrophoresis experiment flown on the shuttle third mission, STS-3. In that experiment a gas bubble was observed occupying the nose of the sample mass causing a distortion of the imposed electric field and subsequent disruption of the experiment. The exact origin of these bubbles is not known and could have been due to a number of reasons, but regardless of their origin, these bubbles did cause problems in performing the experiments.

This problem of unwanted bubbles has become especially acute recently due to the sharp rise in the number of low gravity experiments involving liquid handling procedures which are performed on board the Space Shuttle flights. In their Nucleation of Crystals from Solution experiments (NCS) conducted on USML-1, Kroes et al. (1995), for example, reported that no nucleation took place in the first run of their experiment due to the presence of a number of large air bubbles within the nucleation liquid. In a different experiment involving liquid deposition on solid surfaces, Trinh and Depew (1994) indicated that the bursting of an wanted bubble caused the test liquid to spread beyond the predesigned pinning edge rendering that particular test useless. The same authors discuss encountering major problems with bubbles throughout that experiment.

The problem of gas bubble formation during microgravity liquid handling has been especially serious in most of the Protein Crystal Growth Experiments (PCGE)

conducted aboard the Space Shuttle (1993). This is due to two factors; one, is the large number of protein crystal experiments being performed, which is virtually on every flight of the Space Shuttle. The other is due to the intrinsic nature of protein crystal experiments in which minute liquid volumes are handled. One example is cited in DeLucas et al. (1994) where unexplained bubble formation was observed while extruding solutions from syringes and when filling syringes during execution of PCG experiments within the Glovebox facility on the USML-1 Shuttle mission. Bubbles appeared on the walls of initially dry syringes during the filling process, and had to be removed by manually centrifuging the syringes. During extrusion of solutions from syringes, bubbles also appeared at the exit tip of the needles. The bubbles were suppressed by greatly reducing the extrusion rate, thus wasting valuable time. In this case a special syringe had to be designed to minimize bubble formation during liquid withdrawal. Another incident involved an observation by the Shuttle Glovebox operator in which a needle tip accidentally scraped the bottom surface of a test cell containing the host liquid. In that incident bubbles were observed to form in the liquid immediately after the needle contacted the solid surface. When the same incident was repeated under controlled conditions in the laboratory, no bubbles were observed.

In all of the examples cited above, gas bubbles were generated by gas entrainment during performance of a liquid handling procedure, such as filling an empty vessel with liquid or mixing of liquids. In the Oscillatory Thermocapillary Flow Experiment (OTFE) conducted aboard the USML-1, unwanted bubbles were generated by a boiling process due to spot heating of the host liquid. Kamotani et al. (1994) reported observing bubbles being generated and subsequently developing to large sizes when the temperature of a heater element rose above 60°C. The presence of these bubbles did not only disturb the flow but created a secondary thermocapillary flow around them. The bubbles persisted even after several attempts to remove them from the liquid host were made. Unwanted bubbles also appeared and interfered with PCGE operations during the recently completed USML-2 Shuttel mission. Unwanted bubbles also appeared and iterfered with PCG operations during the recently completed USML-2 Space Shuttle mission.

About 2 years ago an extensive experimental program was initiated for the purpose of understanding the mechanisms leading to bubble generation during fluid handling procedures in a microgravity environment. Several key fluid handling procedures that are typically executed during PCG experiments were identified for analysis in this program. The experiments were designed specifically to understand bubble formation mechanisms during these procedures. The experiments were then conducted aboard the NASA KC-135 aircraft which is capable of simulating a low gravity environment by executing a parabolic flight attitude. However, such a flight attitude can only provide a low gravity environment of approximately $10^{-2}g_0$ for a maximum period of about 20 seconds, in which case all of the tests performed were designed to be completed in under 20 seconds.

Gas bubbles are formed within liquid bulks in either one of two mechanisms; either by gas entrainment into the liquid through the gas/liquid free surface, or by nucleation and diffusion of the dissolved gases within the liquid bulk. Bubbles may be formed by gas entrainment whenever a free gas/liquid interface is punctured such as might happen when surface waves developing on the interface are amplified and subsequently broken. This may occur during filling of an empty container with liquid under highly turbulent flow conditions. Bubbles can also develop by nucleation from a vapor pocket seed through either homogeneous or heterogeneous nucleation. In the homogeneous nucleation case, the vapor seed is formed due to random molecular action within the liquid under the proper thermodynamic conditions. Homogeneous nucleation may occur whenever the pressure within the liquid falls below the vapor pressure, or the temperature rises above the saturation temperature. Heterogeneous nucleation is usually initiated by trapped gas pockets in crevices at solid walls which are in contact with the bulk liquid.

The main mechanisms for bubble generation that are possible during protein crystal growth experiments are either due to cavitation or due to entrainment. Several key fluid handling procedures that involves both of these mechanisms were identified for low gravity experiments and flown aboard the KC-135 aircraft during multiple low-g periods. These include submerged jet cavitation, vessel filling, jet impingement on a solid wall, attached drop growth, and geysering. These experiments are discussed in detail below including the justification, the procedure adopted in tests and the results of the tests.

2. Vessel Filling Experiment

The objective of the tests for the vessel filling experiment was to verify the observations made during the NCS experiments on board the Space Shuttle/USML-1 flight. In that experiment bubbles were observed to develop within the liquid at all of the originally designed liquid inflow rates. The vessel used in the original NCS experiments was also used for the KC-135 tests for the purpose of validating the original observations. In that experiment the inflow tube was positioned along one of the chamber's vertical corners with the exit nozzle next to the cell floor. Two exit nozzle diameters were used for the tests in these experiments; 18 and 14 gauge stainless steel hypodermic needles corresponding to 1.6 and 1.2 mm ID, respectively. Each needle used had either a flat or a beveled tip. Three liquid inflow rates were tested for these experiments: 3.7, 2.0, and 0.5 ml/s. Again, all of the NCS filling experiment tests were conducted during the low gravity portion of each parabola. The primary data acquisition technique for all of the tests performed on board the NASA/KC-135 employed high speed movie camera and film for the purpose of documenting the fluid flow field. Figure 1 shows a sketch of the test cell used for this experiment.

The exiting liquid in the case of high inflow rates was observed to spread along

two paths. One path was along the base of the test cell in which the liquid formed a very thick film with the liquid front advancing radially from the exit corner. The second path of the liquid was along the two vertical side walls adjacent to the exit nozzle (the exit nozzle in all of these tests was located at the bottom corner of the test cell). In this case the liquid took the configuration of hemispherically shaped growing drops propagating along the cell sidewalls. Also, the incoming liquid was observed to climb along the outside of the inlet tube in the cell corner, eventually spreading along the top surface of the cell. Eventually, the accumulating liquid in these tests developed into an hourglass shape in which two large fluid masses formed on the top and bottom surfaces and were connected by a liquid bridge forming along the external surface of the injection tube. Liquid was drawn away from the nozzle due to capillary action along the edge and the tube, consequently partially uncovering the nozzle and allowing air to be entrained at th einterface. Needless to say, that for such a complex gas/liquid interface configuration, a large number of bubbles were engulfed into the liquid, untill it finally became full of bubbles which were evenly distributed throughout the liquid. In the low flow rate tests, the liquid took the configuration of a uniform hemispherical drop forming at the exit nozzle tip. The drop expanded uniformly in the radial direction with further liquid injection. The liquid mass geometry in this case was increasingly symmetric for lower liquid inflow rates. The spherical geometry of the liquid mass is the theoretical limit for zero gravity. The number of engulfed bubbles in all of these tests decreased with decreasing flow rates.

The conclusion that can be drawn from the vessel filling tests is that the geometry of the liquid spread becomes very dependent on capillary effects which becomes more complicated with increasing liquid injection rates. The higher filling rates gave rise to very complex gas/liquid interfaces which quickly became unstable and subsequently broke in response to the dynamics of the liquid motion. The breakup of the free surface naturally led to bubble entrainment within the liquid bulk. In the low filling rate tests the gas/liquid interface developed a shape close to the theoretically predicted spherical geometry which was highly stable. In this case the larger the drop volume the more unstable the interface was. In the stable configuration the free surface did not easily break and thus no bubbles were generated during the filling process. The general tendency for the liquid was to adhere to the adjacent walls and outer surface of the inflow tube except at the corner closest to the inlet nozzle which remained without liquid. Thus in all of the cases tested, a gas bubble was always trapped at the filling corner of the vessel which subsequently became a source for additional bubbles in the liquid bulk as smaller bubbles sheared off the larger one due to the stresses generated by the liquid motion.

3. Submerged Jet Cavitation Experiment

Most of the PCG Space Shuttle experiments involve liquid handling operations using hypodermic needles for either withdrawing liquid from, or injecting liquid into

bulks. The possibility of bubble generation due to cavitation mechanism during these procedures was investigated in the submerged jet cavitation experiment. The cavitation phenomenon occurring due to a submerged jet is an active area of research. Although the physics of the phenomenon does not explicitly involve the effects of the acceleration due to gravity, never the less, a set of tests were designed to explore this phenomenon under low gravity conditions.

It is well known that cavitation can occur in the case of a submerged jet whenever the cavitation incipience index, λ_i is above a critical value. The cavitation inception index is basically a nondimensionalized pressure differential which is normally defined in the following manner:

$$\lambda_i = \frac{P_{\infty i} - P_v}{0.5\rho V_j^2}$$

where $P_{\infty i}$ is the ambient liquid pressure, P_v is the vapor pressure, ρ is the liquid density, and V_j is the jet exit velocity. The cavitation inception index is an empirical parameter which depends on many variables, including the jet diameter and the properties of the liquid. Data from a number of experiments measuring the cavitation index for submerged water jets are summarized in Ran and Katz (1994) as a function of the nozzle diameter. The tests in the present low gravity experiment were tailored to investigate the effects of gravity on the value of λ_i. In these tests two different gauge hypodermic needles were used for producing the jets; namely 15 and 18 gauge needles corresponding to 1.6 and 1.2 mm ID, respectively. Four different jet inflow rates were tested in these experiments corresponding to 94, 80, 60 and 40 ml/min, allowing the use of four different jet exit velocities for each needle. These flow rates were designed to encompass exit velocities that correspond to the critical values for λ_i in the data summarized by Ran and Katz. A high speed camera operating at 400 frames/s was used to identify any gas bubbles that may develop during each test. Figure 2 shows a sketch of the test cell designed for investigating the submerged jet cavitation experiment.

All of the submerged jet cavitation tests that were conducted did not show any bubbles forming in the vicinity of the jet exit nozzle. This was expected since the test hardware design criteria for jet diameters and jet exit speeds, were below the critical values for cavitation to take place. These tests were repeated in the second flight campaign in which the jet conditions were brought closer to the critical values. Again, no cavitation bubbles were observed in the second flight experiment. It is possible to conclude from these tests that the magnitude of the gravitational acceleration plays no role on the value for λ_i a long as the exit velocity is below the critical value.

4. Solid Surface Scratch Experiment

The purpose of the solid surface scratch experiment was to investigate the bubble generation mechanism encountered during accidental scraping of the protein crystal-

lization instrument by the spaceflight operator on board the USML-1 space shuttle flight. The tests for these experiments were conducted manually by the KC-135 flight experiment operator during the low gravity portion of each parabola. These tests were very simple in that a stainless steel hypodermic needle was manually inserted through a septum port installed at the top of the test cell and was made to scrape along the desired test surface. For each test, the cell was partially filled with the test liquid such that the liquid level was at least 10 mm above the surface to be scratched. The different surfaces that were tested were glued to the bottom inner surface of the cell. Again, a high speed movie camera and film was used to record the motion of the needle during the scrapping action and also to record the formation and development of the ensuing bubbles. Figure 3 shows a sketch of the test cell used for conducting this experiment.

Bubbles were observed to form during the scrapping action in most of the tests recorded. It was also observed that bubbles formed only when the scrapping action was jerky. In other words when the scrapping needle motion was uneven such that the tip was skipping over the solid surface. No bubbles were observed to develop when the scrapping motion was smooth and gentle. The bubble formation was found to be independent of the PEG concentration of the liquid, the type of surface scrapped.

Careful analysis of the scratch tests led to the conclusion that the gas bubbles observed during the scrapping action must have been entrained through the gas/liquid free surface with the assistance of the needle. The actual mechanism of bubble generation appear to be due to the oscillation of the needle as it momentarily sticks and skips along the scratch surface when it is caught along the solid surface and then released and swings forward. The bubble formation mechanism was not due to the scrapping action but due to the oscillation of the needle across the gas/liquid free surface during the motion. The thinner and thus more flexible the needle the more likely it will generate bubbles by entraining gas from the gas/liquid interface during each catch and release. This bubble generation mechanism was determined by reducing the film frame rate to 6 frames per second and then further to a single frame observations. This was necessary since the gas entrainment mechanism occurred in these tests extremely fast. The single frame analysis of the tests shows very clearly that a fast oscillation of the needle tend to engulf gas from the downstream side of the needle at the gas/liquid interface and then down into the liquid bulk along the needle axis. The gas is initially entrained in the form of a cloud, surrounding the submerged portion of the needle, which subsequently breaks up into bubbles. The bubbles will then spread throughout the liquid bulk along the motion streamlines of the liquid. There are two characteristic features of these tests, one is the existence of a lower limit of the needle oscillation frequency below which gas is not entrained. The other feature is the speed with which gas is entrained. The gas cloud was observed to form during a single frame advance of a 400 frames/s shot indicating that it occurred in under 2.5 milliseconds.

5. Jet Impingement Experiment

This experiment was designed to investigate the spreading mechanism of a liquid jet over a solid surface upon impacting the surface. Jet impingement is a fluid handling procedure that could develop during filling of a vessel when the inflow rate is very high and the receiving vessel is small. It is obvious that the liquid spread over the solid surface resulting from a jet impact in low gravity environment is entirely different from a similar incident under terrestrial conditions. In a terrestrial laboratory the spreading mechanism depends very strongly on the orientation of both the jet and the solid surface. Such dependence on surface orientation is absent in low gravity environment. Another objective of this experiment was to delineate the conditions under which some of the impacted liquid rebounds from the solid surface in the form of droplets that subsequently fold gas bubbles into the liquid bulk.

The test cell for this experiment comprised of a plexiglas cubical box with the dimensions of 2.5 cm on each side. A hole was drilled at the center of one of the cube faces, through which a hypodermic needle was inserted. The needle end was positioned at a set predetermined distance from the opposite wall. The liquid jet in each test for this experiment was established by injecting liquid through the hypodermic needle. The impact of the jet on the opposite face of the cube and the subsequent accumulation and spreading of the liquid on the wall was visually recorded using high speed motion picture camera. The liquid flow rate was achieved using a syringe pump capable of delivering the test liquid at a constant rate with a preset flow rate setting. Figure 4 shows a sketch of the test cell used for performing this experiment.

The objective of this experiment was to understand the mechanism of jet impact on a solid wall and the subsequent geometry development of the liquid spreading for different jet exit velocities, different tets liquids and different liquid jet lengths. Two hypodermic needle sizes were used in these tests one with 0.16 cm ID and another with 0.12 cm ID. Four test liquid types were used for this experiment; distilled water, and a mixture of water with 10% PEG, 20% PEG, and 30 % PEG, respectively. Four different jet lengths were tested: 0.5 cm, 1.0 cm, 1.5 cm and 2.0 cm. Flow rates of 20, 30, 40 and 50 ml/min were used corresponding to jet exit velocities of 25, 30, 40, 45, 60, and 74 cm/sec.

Each test was initiated after the low gravity portion of the aircraft flight parabola was attained by activating the pump and the camera. Most of the tests had a liquid injection period no longer than 5 seconds. Each test was completed during the low gravity period of the parabola. Normally only one test was conducted during a single parabola. Also every test was performed at least twice, once with a dry wall initial conditions and another with a wet wall initial conditions. For each test one of the four variables, namely, the flow rate, the needle diameter, the test liquid type, or the jet length was varied while the rest of the parameters were kept constant. This experiment was performed in the second and third KC-135 flights campaigns which

took place during June 20 - 24, 1994 and January 30 - February 3, 1995. Table I shows all of the tests performed on board the KC-135 aircraft for this experiment.

The results of the tests for this experiment show that the tendency of the liquid is to always accumulate at the jet impingement point with the solid wall. At a dry wall the accumulating liquid took the form of a hemispherical dome with its cap at the jet end and the flat surface against the solid wall. As more liquid was injected, the dome expanded radially increasing both its base and its height. This form of liquid accumulation was consistent regardless of the jet exit velocity, the jet diameter, or the type of test liquid used. The liquid spread over the solid surface was manifested, in this case, through an expansion of the base of the liquid dome in the radial direction. This was the accumulation configuration observed whenever the wall was dry.

When the liquid jet impacted a wet wall the liquid spreading configuration varied from test to test depending on the shape of the original liquid film on the solid wall prior to the jet impact. In this case the liquid meandered along the wet region of the wall after some liquid mass accumulated at the stagnation region. However, the liquid meandered only after it acquired some mass and when gravity perturbations were present. In other words the accumulating liquid mass was very unstable to small disturbances when the wall was wet. The meandering liquid mass took very interesting forms and shapes which are not the subject of this experiment. No splattering of liquid was ever observed for all jet exit velocities tested in this experiment.

The flow of the liquid over the solid surface after impact was extremely interesting, forming unusual patterns that can only be observed under low gravity conditions. One of the most common patterns observed was the motion of the hemispherical dome along the wet path of the wall and also the merging of accumulating liquid volume with existing volume shapes in the container. The resulting liquid configuration took different shapes depending on the material it merged with. In certain instances the hemispherical drop merged with a horizontally flat gas/liquid interface. This pattern evolved as the liquid accumulated from the jet impact on the wall, spread, and subsequently collided with another liquid volume already inside the container, when it was partially filled with liquid. In other instances when the test chamber was empty the hemispherical drop evolved into a quarter spherical shape located at the intersection of two walls of the test chamber.

6. Sessile Drop Growth Experiment

The purpose of this experiment was to investigate the growth process of a drop attached onto a solid surface as liquid was being continuously added to the volume. The growth process of the attached drop includes in this case the development of the drop geometry with increasing liquid mass as well as the variation of the liquid/solid contact angle as the drop spreads along the solid surface.

TABLE I

Needle Gauge	Jet Dia mm	Jet Length mm	Flow Rate ml/min	Jet Exit Vel cm/s	Test Liquid
16	1.2	10	30	44.2	Water
16	1.2	20	30	44.2	Water
16	1.2	10	50	73.7	Water
16	1.2	20	50	73.7	Water
14	1.6	10	30	24.9	Water
14	1.6	20	30	24.9	Water
14	1.6	10	50	41.4	Water
14	1.6	20	50	41.4	Water
16	1.6	5	20	29.5	Water
16	1.6	5	30	44.2	Water
16	1.6	5	40	58.9	Water
16	1.6	5	50	73.7	Water
16	1.6	10	20	29.5	10%PEG
16	1.6	10	30	44.2	10%PEG
16	1.6	10	40	58.9	10%PEG
16	1.6	10	50	73.7	10%PEG
16	1.6	15	30	44.2	20%PEG
16	1.6	15	40	58.9	20%PEG
16	1.6	20	30	44.2	30%PEG
16	1.6	20	40	58.9	30%PEG
16	1.6	20	50	73.7	30%PEG

Test Matrix For Jet Impingement Experiment

TABLE II

Nozzle Dia mm	Liquid Flow Rate ml/min	Liquid Exit Vel. cm/s	Test Liquid	Comments
1.6	2	1.66	Water	
1.6	3	2.49	10%PEG	sphere
1.6	4	3.32	20%PEG	
1.6	6	4.98	30%PEG	disc
1.2	2	2.95	Water	sphere
1.2	3	4.43	10%PEG	sphere
1.2	4	5.9	20%PEG	
1.2	6	8.85	30%PEG	
1.2	14	20.63	Water	
0.84	2	6.04	Water	
0.84	3	9.06	10%PEG	
0.84	4	12.08	20%PEG	
0.84	6	18.12	30%PEG	
0.84	14	44.1	Water	geyser
0.58	2	12.6	Water	
0.58	3	18.9	10%PEG	
0.58	4	25.2	20%PEG	
0.58	6	37.8	30%PEG	
0.58	14	92.42	Water	geyser

Test Matrix For Dynamic Wetting Experiment

All of the tests for this experiment were conducted by injecting liquid through a hole drilled into a solid surface. The liquid drop was formed by injecting liquid through the hole. The drop subsequently was allowed to remain attached to the surface. The test cell for this experiment comprised of a plexiglas cube of 2.5 cm per side. The hole was drilled at the center of one of the cube faces. Liquid was supplied to the drop using a hypodermic needle attached to the external surface of one of the test cell walls. Four different needle sizes were used for injecting the liquid with the following ID's: 0.16, 0.12, 0.084, and 0.058 cm, respectively. Five liquid injection flow rates were used resulting in liquid exit velocities ranging from 1.66 cm/sec to 92.4 cm/sec, depending on the needle diameter. Also, four different liquid types were used in these tests including distilled water, distilled water solution with 10% PEG, 20% PEG, and 30% PEG, respectively. The growth of the drop was recorded visually using high speed movie camera and film. Figure 5 shows a sketch of the test cell used for this experiment.

Each test in this experiment was initiated by injecting liquid through the orifice in the solid surface at a constant flow rate. The variation of the shape of the drop was recorded visually as additional liquid is injected. Each test was conducted during the low gravity portion of the flight parabola. The liquid flow rates, the test liquid and the pore size were varied separately for each individual test. Table II lists all of the tests performed on board the KC-135 aircraft for this experiment.

Altogether there were 20 different successfully completed tests in this experiment over the second and third KC-135 flight campaigns. In all of the tests for which the liquid exit velocity was higher than 40 cm/sec, the liquid issued from the orifice in the form of a jet and consequently a liquid drop did not form at the orifice. For all of the tests in which the liquid exit velocity was lower than 40 cm/sec a drop was observed to form and develop in almost identical manner for all of the tests except in three cases. In the majority of the tests the liquid drop took an almost perfect hemispherical domed shape immediately upon exiting the orifice with its flat surface against the solid wall. The drop was attached to the orifice in all of these cases and was positioned centrally at that location. As further liquid was added to the drop, the drop expanded radially while retaining its hemispherical shape. However, in one test for which the conditions were: 0.16 cm orifice diameter, 4.98 cm/sec for the exit velocity, and 30% PEG test liquid, the hemispherical dome flattened out to a disc covering the orifice as the liquid mass increased beyond a specific value.

In the remaining three cases, for which the orifice diameter and exit velocity were: 0.16 cm and 2.49 cm/sec; 0.12 cm and 2.95 cm/sec; and 0.12 cm and 4.3 cm/sec, respectively, the liquid took an almost perfect spherical shape upon exiting the orifice with the drop being attached to the orifice at a single point. The spherical drop expanded radially with increased injection of the test liquid which was distilled water in all of the three cases. However, the spherical shape became unstable as further liquid was injected and subsequently the drop shape was altered to a hemispherical dome as it wets the surface. The cause of this shape instability could either have been due to the

effects of the residual gravity or to the increased mass of the drop. The specific cause for this instability could not be readily identified since that test run was conducted without the benefit of the accelerometer readings being visible simultaneously with the photograph.

No attempt has yet been made at measuring the variation of the solid/liquid contact angle as a function of the advancing liquid front speed during the growth of the drop. The following general conclusion can be drawn from this experiment. At very low exit velocities, i.e. less than 5 cm/sec the attached liquid drop took a spherical shape. For higher exit velocities a hemispherical domed shape drop was consistently observed.

7. Low Gravity Vessel Experiment

Based upon the low gravity tests performed in two of the previous experiments, namely the Vessel Filling Experiment and the Jet Impingement Experiment, a novel design concept for an efficient low gravity receiving vessel was defined. The basic requirements for such a container is that the accumulating liquid must not be confined within solid walls. The Vessel Filling Experiment tests indicated that the walls of the vessel, and especially the corners, became sites in which bubbles were trapped which may subsequently detach and move within the liquid bulk. This finding coupled with the observation that the liquid issuing from a jet will tend to accumulate in the shape of a hemispherical drop at the point of impact of the jet with the solid wall, led to the design concept of the low gravity vessel. The design of the vessel employes the surface tension force at the free gas/liquid interface as the primary mechanism for holding the liquid volume together. In low gravity environment where the weight of the liquid is negligible, the surface tension force is sufficient to hold a large liquid mass intact. Thus it was concluded that a vessel whose walls are constructed from a wire screen mesh could fulfill these requirements.

Tests on the low gravity vessels, from here on will be called *cages*, were conducted during the third and fourth KC-135 flights using different vessel geometries and materials. The purpose of the tests was to identify the optimum flow rate appropriate for a specific cage geometry and screen mesh gap size. Optimum flow rate is understood within the context of this experiment to mean the maximum flow rate possible for which a stable liquid configuration can exist and within which all of the liquid may be confined within the cage walls.

A special experimental apparatus was designed and constructed specifically for the purpose of testing and investigating these criteria. The experimental apparatus consisted of a plexiglas rectangular containment vessel within which the low gravity cage was suspended. The containment vessel inner dimensions were 9.8 long by 7.0 by 5.7 cm. The plexiglas material for the containment vessel was chosen to allow for visual observation of the vessel filling process. The cage was suspended at the center of the

containment vessel using eight small springs. One end of each spring was connected to an interior corner of the container and the other end to an edge of the cage. The test liquid was injected into the cage using a hypodermic needle with different gauge sizes. The needle was inserted at the center of one flat face of the containment vessel through a septum port installed into one of the vessel walls. The needle was allowed to penetrate through the cage up to 0.5 cm from one of its end faces. A schematic of the experimental apparatus used in these tests is shown in figure 6.

Altogether nine different cages were constructed and tested. Six cages were circular cylindrical in shape 4.6 cm long and 2.6 cm in diameter. The remaining three cages were cubic in shape with 3 cm on each side. Five of the cylinders were constructed from a metal wire mesh material and one from a plastic wire material. Four of the metal cylindrical cages had square weave mesh gaps of 0.27 cm, 0.45 cm, 0.55 cm, and 1.27 cm, corresponding to 1/8, 1/4, 3/8 and 1/2 inches respectively. The remaining metal cage was constructed from a diamond shape weave with 1.06 cm by 0.38 cm gap size. The plastic cylindrical cage was constructed from a plastic mesh screen with a square weave of 0.95 cm gap. Two of the cubic vessels were constructed from metal wire mesh screens with square weave, one with 1.27 cm gap and the other with 0.55 cm gap. The remaining cubical shape cage was constructed from a plastic material with square wave screen having 0.95 cm gap.

The two cage materials tested, namely the plastic and metal, were utilized in order to understand the effects of the liquid/solid contact properties on the liquid holding capabilities of the cages. Also, the different weave shape and size were used to test the stability of the free gas/liquid interface and its effects on the liquid holding properties. Several tests were conducted using a solid cylindrical plexiglas vessel for comparison between the conventional solid walled vessel and the new cage design concept. Specifically, the objective in here was to see whether or not more gas bubbles are trapped in the conventional vessel for the same flow rates and test liquid.

Three test liquids were used in this experiment including distilled water, saline water, and 15% PEG 400 with distilled water. These specific test liquids were chosen to model the various fluids used in the Protein Crystal Growth Experiments in microgravity. Several different flow rates were used in the tests for this experiment ranging from 10 ml/min to 75 ml/min. The test liquid was injected using a syringe pump which is capable of delivering a preset metered flow rate. Several hypodermic syringes were used to allow for higher test liquid flow rates. Since the same hypodermic needle was used to inject the test liquid into each cage or solid vessel tested, the various flow rates are conveniently translated into jet exit velocities ranging from 8 cm/sec to 80 cm/sec. Table III lists the parameters for all of the low gravity tests performed for this experiment.

TABLE III

Vessel Geom.	Mesh Size mm	Mesh Mater.	Flow Rate ml/min	Jet Exit Vel cm/s	Test Liquid
Cylind	2.7	Metal	10,20,30,40	8.3,16.6,25,33	Water
Cylind	4.52	Metal	20,30,40,50	16.6,25,33,41	Water
Cylind	5.5	Metal	20,30,40,50	16.6,25,33,41	Water
Cylind	5.5	Metal	45,60,75	37,50,82	Water
Cylind	5.5	Metal	45,60,75	37,50,82	15%PEG
Cube	5.5	Metal	45,75	37,82	Water
Cube	5.5	Metal	45,60,75	37,50,82	15%PEG
Cylind	9.46	Plastc	45,60,75	37,50,82	Water
Cylind	9.46	Plastc	45,60,75	37,50,82	15%PEG
Cylind	9.46	Plastc	45,60,75	37,50,82	Saline
Cube	9.46	Plastc	30,45,60	25,37,50	Water
Cube	9.46	Plastc	30,45,60	25,37,50	Water
Cylind	12.7	Metal	30,45,60	25,37,50	Water
Cylind	12.7	Metal	30,45,60	25,37,50	Saline
Cylind	12.7	Metal	30,45,60	25,37,50	15%PEG
Cylind	Diamond 10.6/3.8	Metal	20,30,40,50	16.6,25,33,41	Water

Test Matrix For Low Gravity Vessel Filling Experiment

The flow field developing due to the inflow of the test liquid into each cage was recorded visually using high speed photographic camera and film. Two film speeds were used: 400 frames/sec and 250 frames/sec. One parabola was used for each injection test with a typical low gravity period of up 20 sec. Also, a readout of the aircraft acceleration values in micro-g levels during each parabola was attached below the test vessel in order to allow for observing the fluid behavior simultaneously with the actual acceleration values.

The results from the vessel filling tests revealed that the liquid accumulation pattern within each cage depended to a large extent on the jet exit velocity. At the lowest values for the jet exit velocities tested, i.e. $V_j \leq 20$cm/sec, the exiting liquid accumulated as a drop and attached to the cage frame in the vicinity of the nozzle. The liquid drop grew in size as the liquid injection continued. During its growth the liquid drop remained attached to its initial attachment point. However, the unattached free surface was observed to wobble and move in response to variations in the aircraft's acceleration vector magnitude and direction. The liquid drop remained stable in its original position up to $\approx 0.1 g_0$. As the magnitude of the acceleration vector increased beyond this value the liquid began to drain from the vessel frame and into the containment vessel.

For jet exit velocities of 20 cm/sec $\leq V_j \leq$ 40 cm/sec, The liquid jet tended to impinge on the far side of the cage frame. Upon impingement, the liquid adhered to the inside surface of the cage frame in the form of a drop. With further injection of liquid, the liquid volume grew from the far side towards the the nozzle end and remained within the cage frame as the liquid accumulation increased. For exit velocities greater than 40 cm/sec the jet penetrated through the wire mesh at the opposite end of the cage whenever the jet diameter was much smaller than the mesh gap. However, when the mesh gap was of the same order as the jet diameter, the liquid had greater tendency to be captured by the cage frame and subsequently accumulate at that location. When the jet diameter was smaller than the mesh gap, if the jet struck the mesh the liquid tended to *grab-on* and stick to the wire and grow back into the cage from that point. Whether or not the jet attached to the wire depended only on the jet velocity.

8. Free Surface Vibration

The solid surface scratch experiment described in section 4.0 revealed that the source for the observed bubbles was the breakup of the free surface and bubbles were not generated at the solid surface. In other words, the bubbles were actually entrained from the free surface and did not originate at the tip of the needle as it scratched the bottom submerged surface of the container. However, the results from that experiments were qualitative in nature and it was decided that further investigations were needed in order to quantify the exact mechanism responsible for bubble entrainment in this case. To this end the free surface vibration experiment was defined in which a hypodermic needle, which was immersed into the liquid normal to the free surface, was made to

oscillate in the direction parallel to the free surface. This method of oscillation of the free surface can lead to its breakup when the appropriate oscillation frequency and amplitude were applied. Different tests were performed for this experiment in which the frequency and amplitude of vibration were varied. The objective of this experiment was to delineate the frequency and amplitude boundaries of vibration that gave rise to bubble entrainment into the liquid.

The test cell for this experiment was constructed from plexiglas material in the shape of rectangular container which was 2.5 cm high, 2.5 cm wide and 2.5 cm deep. The test cell was filled with the test liquid up to prescribed height before performing each test where the vibrating needle was allowed to penetrate through the free surface up to 10 mm below the surface. Figure 7 shows a sketch of the test arrangement for this experiment. Each test was performed by allowing the needle to oscillate in the direction parallel to the free surface during the low gravity interval of the flight parabola. The vibrating needle was bent into a 90^o angle and was glued to a loud speaker diaphragm and was made to vibrate by activating the speaker. The speaker was connected to a signal generator and an amplifier. The vibration frequency and shape were established by the signal generator while the vibration amplitude was controlled through the power setting of the amplifier. A high speed camera was used to record visually the fluid behavior at the free surface during each test using high speed film. Two different test liquids were used with several amplitude and frequency settings.

The tests for this experiment were performed on two separate KC-135 flight campaigns, the first during January 30 - February 3, 1995, and the second during April 10 - 14, 1995. In the first flight, only distilled water was used for the test liquid in which five frequencies were tested, namely 50, 78, 125, 175 and 200 Hz, with four power settings for each frequency tested. The results of these tests showed that bubbles were generated and entrained into the liquid as a consequence of the needle oscillation at only one frequency, the 78 Hz frequency and for all power settings. No bubbles were observed to form for all other frequency settings. The 78 Hz oscillation frequency is the resonant frequency for that experiment configuration and as such had very large amplitudes. Also the needle was oscillating at an angle to the free surface at that frequency.

In the second flight campaign a larger liquid container and four test liquids were used; distilled water and distilled water with 10, 20 and 30% PEG solutions. In this flight only two frequencies were used in the experiment, namely 48 and 94 Hz with the similar four power settings as tested in the previous flight. The two frequencies used in this experiment were also the resonant modes for this experimental configuration. Being the resonant frequencies all of the tests generated a large number of bubbles.

9. Conclusions

The experimental program described above was conducted in order to understand the

mechanism by which bubbles develop within the liquid during fluid handling procedures executed in PCGE in low gravity environment. This problem is unique to low gravity environment since rarely bubbles are found to be lodged within the liquid host in terrestrial environment. This difference in bubble behaviour between low gravity and terrestrial conditions is solely due to the decrease or absenece of the bouyancy force in the former. To this end a series of experiments were designed to model typical liquid handling procedures in PCGE. A number of typical procedures were investigated in depth in these expeiments including filling of an empty vessel with liquid, liquid expulsion from a vessel, and mixing of liquids. In addition, several modes of vessel filling procedures were studied in these experiments.

The experiments were designed to be conducted on board the NASA/KC-135 aircraft which is capable of providing up to 20 seconds of $\pm 10^{-2} g_0$ in gravitational acceleration. Results from all the low gravity tests revealed that all of the bubbles which were found to develop within the liquid host, and which were not initially present in the liquid, were entrained into the liquid through the gas/liquid free surface. The cause of bubble entrainment was the rupture of the free surface itself. The free surface can breakup either due to turbulence in the free surface or due to breakup of waves developing on the surface. The results of these tests show that gas bubbles entrainment can be effectively reduced through careful management of the fluid motion during liquid handling procedures so as to prevent turbulent flow development or to suppress surface wave amplifications. Both of these processes dictates that all fluid motion resulting from fluid handling procedures must be forced to be very slow.

Also, when filling an empty container with liquid it was found that any vessel corner can act as a source for bubble generation. This was found to occur due to the inability of the liquid initially to completely wet the container corner and thereby leaving a gas bubble trapped at that location. Gas bubbles can subsequently be sheared away from the corner bubble and subsequently move within the host liquid through fluid advective motion. This problem can be adequately resolved by substituting the solid vessel material with an open weave mesh material. The preliminary tests described above on the low gravity vessel filling experiments clearly show that the open weave mesh vessel wall can resolve the problem of bubble entrapment in vessel corners.

10. References

Bier, M., Snyder, R.S. etc. "Role of Gravity in Preparative Electrophoresis", Proc. 3rd Space Processing Symp., Skylab Results, Vol. 2, 1974, pp. 729-753.

DeLucas, L.J. Private communication, 1993.

DeLucas, L.J. et al. "Protein Crystal Growth Results from the United States Microgravity laboratory - 1 Mission", in *Joint Launch + One Year Science Review*

of USML-1 and USMP-1 with Microgravity Measurement Group, NASA CP 3272, Vol. 1, 1994, pp. 409-419.

Kamotani, Y., Ostrach, S. and Pline, A. "Oscillatory Thermocapillary Flow Experiment (OTFE)", in *Joint Launch + One Year Science Review of USML-1 and USMP-1 with Microgravity Measurement Group*, NASA CP 3272, Vol. 2, 1994, pp. 701-709.

Kroes, R.L., Reiss, D.A. and Lehoczky, S.L., "Nucleation of Crystals from Solution in Microgravity", *Microgravity Science and Technology*, Vol. 8, pp. 52-55, 1995.

Ran, B. and Katz, J. "Pressure Fluctuations and their Effect on Cavitation Inception Within Water Jets", *J. Fluid Mech.*, Vol. 262, 1994, pp. 223-263.

Snyder, R.S., Rohdes, P.H., Herren, B.J., Miller, T.Y. and Seaman, G.V. "Analysis of Free Zone Electrophoresis of Fixed Erythrocytes Performed in Microgravity", *Electrophoresis*, Vol. 6, 1985, pp. 3-9.

Trinh, E.H. and Depew, J. "Solid Surface Wetting and Deployment of Drops in Microgravity", in *Joint Launch + One Year Science Review of USML-1 and USMP-1 with Microgravity Measurement Group*, NASA CP 3272, Vol. 2, 1994, pp. 583-600.

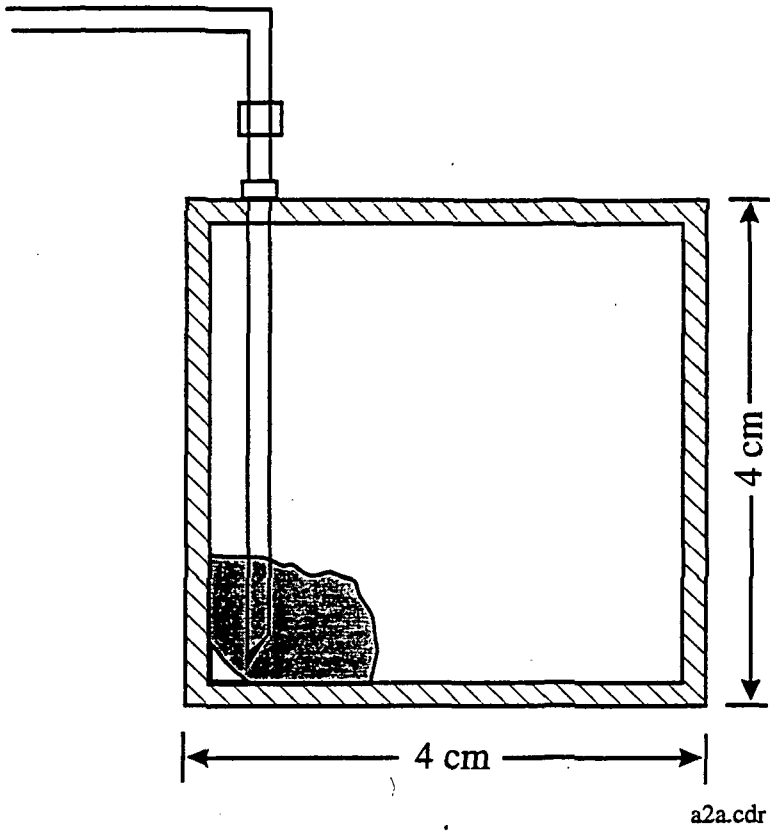

Figure 1. Sketch of the test cell used for the vessel filling experiment.

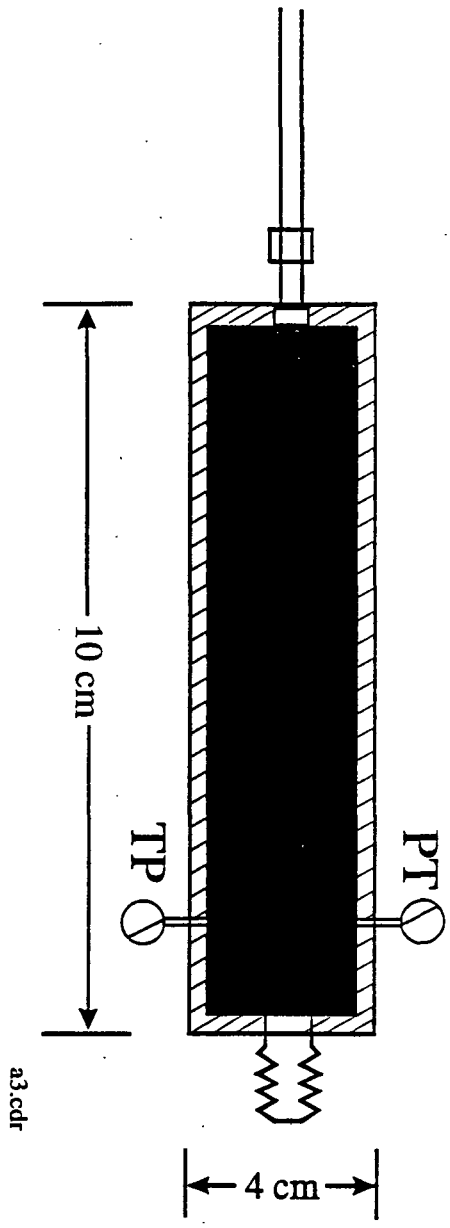

Figure 2. Sketch of the test cell used for the submerged jet cavitation experiment.

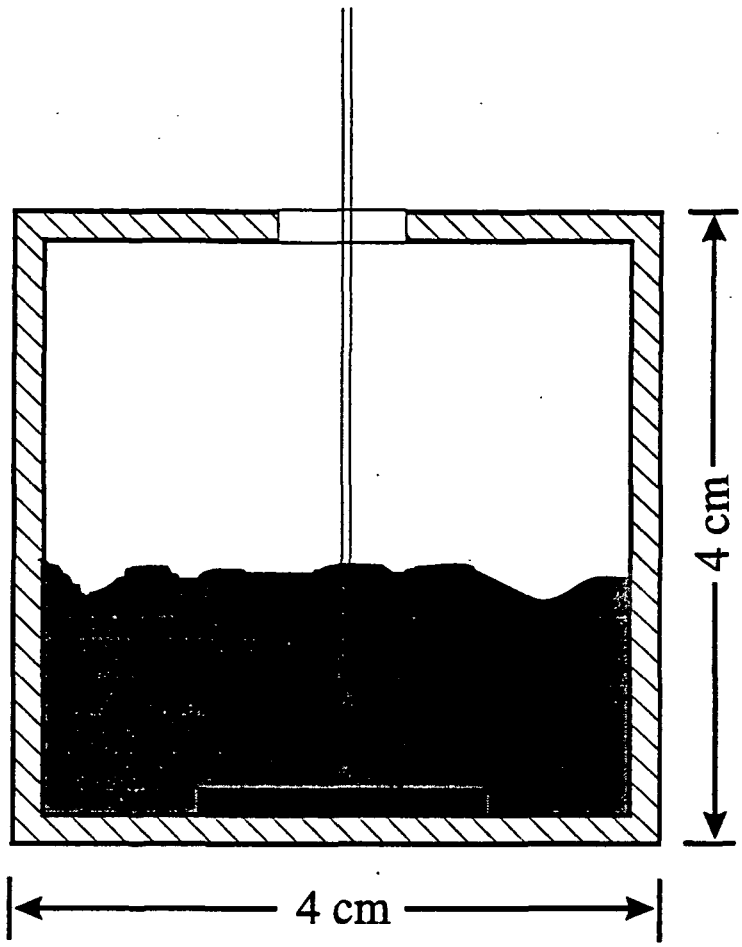

Figure 3. Sketch of the test cell used for the surface scraping experiment.

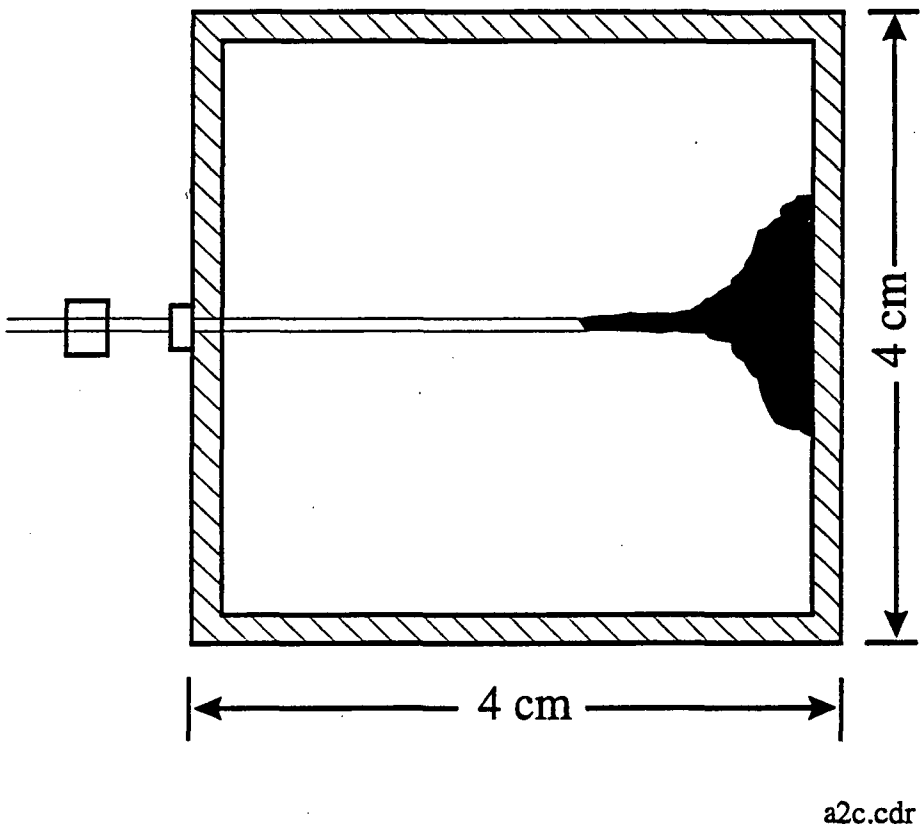

Figure 4. Sketch of the test cell used for the liquid jet impingement experiment.

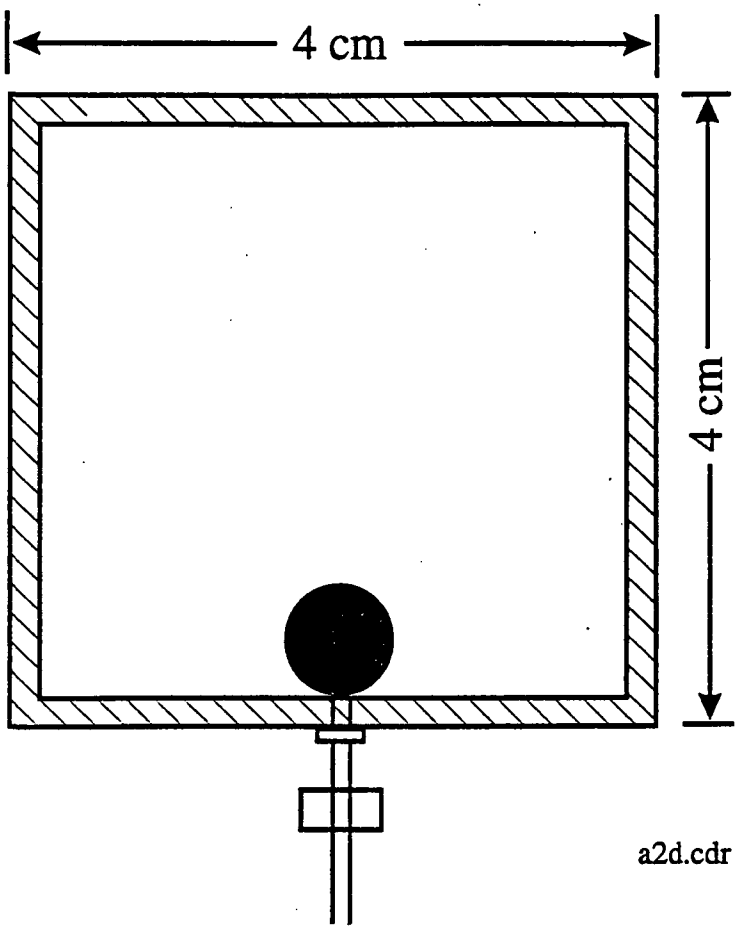

Figure 5. Sketch of the test cell used for the attached drop growth and geysering experiments.

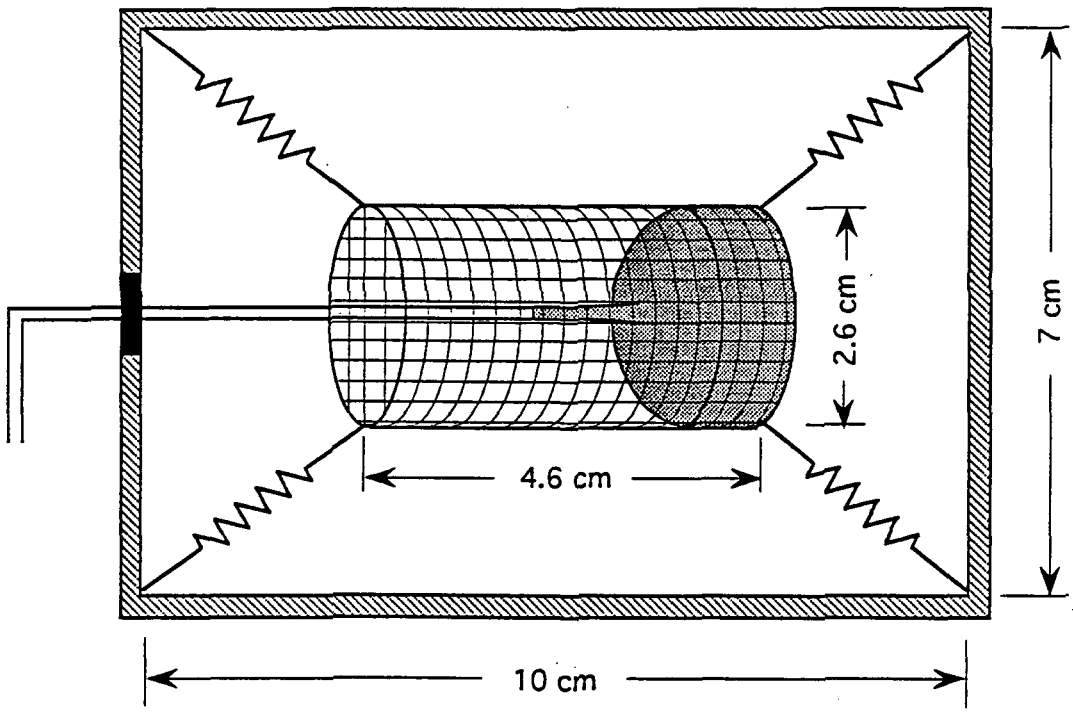

Figure 6. Sketch of the test cell used for the low gravity vessel experiment.

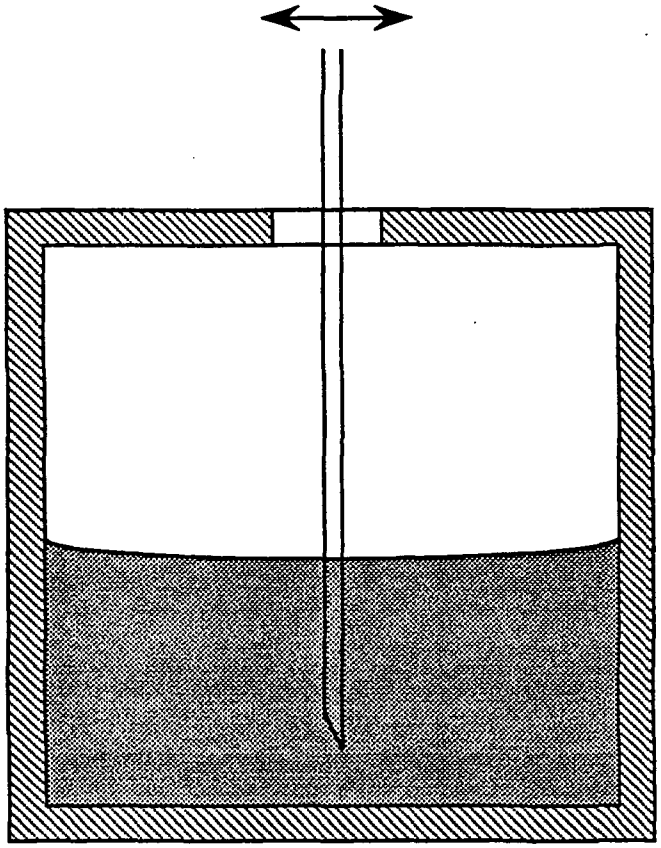

Figure 7. Sketch of the test cell used for the surface breakup experiment.